



## Research article

# Silencing of TXNIP attenuates oxidative stress injury in HEI-OC1 by inhibiting the activation of NLRP3 and NF- $\kappa$ B

Ning Ma <sup>a,1</sup>, Liang Xia <sup>b,c,d,1</sup>, Zhong Zheng <sup>b,c,d</sup>, Xiaoyan Chen <sup>b,c,d</sup>, Weiwei Xing <sup>e,\*</sup>, Yanmei Feng <sup>b,c,d,\*</sup>

<sup>a</sup> Post Graduate Training Base of Jinzhou Medical University in Shanghai Six People's Hospital, Jinzhou, China

<sup>b</sup> Department of Otolaryngology–Head and Neck Surgery, Shanghai Sixth People's Hospital Affiliated to Shanghai Jiao Tong University School of Medicine, Shanghai, China

<sup>c</sup> Otolaryngology Institute of Shanghai Jiao Tong University, Shanghai, China

<sup>d</sup> Shanghai Key Laboratory of Sleep Disordered Breathing, Shanghai, China

<sup>e</sup> Department of Otolaryngology–Head and Neck Surgery, First Affiliated Hospital of Jinzhou Medical University, Jinzhou, China

## ARTICLE INFO

## Keywords:

SNHL  
TXNIP  
Oxidative stress  
HEI-OC1  
NLRP3  
NF- $\kappa$ B

## ABSTRACT

Sensorineural hearing loss (SNHL) is the most common type of hearing loss worldwide. The primary mechanism is oxidative injury to the cochlea as a result of oxidative stress. Therefore, exploring antioxidant strategies is particularly important in addressing SNHL. Thioredoxin-interacting protein (TXNIP) is an upstream target of oxidative stress-induced damage, and the NOD-like receptor protein 3 (NLRP3) and NF- $\kappa$ B pathways may be the main downstream molecular pathways, but this has not been reported in SNHL. Therefore, we investigated the molecular mechanism and role of TXNIP in oxidative stress injury induced by H<sub>2</sub>O<sub>2</sub> in the HEI-OC1 auditory cells. To induce oxidative stress, HEI-OC1 cells were treated with H<sub>2</sub>O<sub>2</sub>. The TXNIP expression was measured by western blotting and immunofluorescence. Intracellular TXNIP was knocked down using small interfering RNAs (siRNAs). Cell viability was measured by CCK8, total intracellular reactive oxygen species (ROS) by DCFH-DA, mitochondrial ROS by Mito-SOX, NLRP3, pro-caspase-1, total p65 NF- $\kappa$ B, and phospho-p65 NF- $\kappa$ B expression were measured by western blotting. Statistical analyses were performed using one-way analysis of variance, and  $p < 0.05$  was considered statistically significant. We found that H<sub>2</sub>O<sub>2</sub> treatment induced oxidative stress injury in HEI-OC1 cells, as evidenced by decreased cell viability and increased total intracellular and mitochondrial ROS levels ( $p < 0.05$ ). TXNIP expression was elevated, and NLRP3 and NF- $\kappa$ B were activated ( $p < 0.05$ ). Moreover, siRNA-TXNIP co-treatment reversed these changes and protected HEI-OC1 cells from oxidative stress ( $p < 0.05$ ). We concluded that H<sub>2</sub>O<sub>2</sub>-induced oxidative stress in HEI-OC1 cells was alleviated by TXNIP inhibition. The finding may provide new insight into the prevention and treatment of SNHL.

\* Corresponding author. Department of Otolaryngology–Head and Neck Surgery, Shanghai Sixth People's Hospital Affiliated to Shanghai Jiao Tong University School of Medicine, Shanghai, China.

\*\* Corresponding author.

E-mail addresses: [lxingweiwei@163.com](mailto:lxingweiwei@163.com) (W. Xing), [yymfeng@sjtu.edu.cn](mailto:yymfeng@sjtu.edu.cn) (Y. Feng).

<sup>1</sup> These authors contributed equally to this work.

## 1. Introduction

Hearing loss is the most common sensory impairment disease, which affects people of all ages. The World Health Organization has predicted that more than 5 % of the world's population currently suffers from hearing loss, and this is estimated to rise to 10 % of the world's population by 2050 [1]. The most common type of hearing loss is sensorineural hearing loss (SNHL), which includes hereditary, drug-induced, and noise, and age-related hearing loss. The main pathological feature of SNHL is damage to hair cells, which are sensors of the cochlear conduction pathway that cannot regenerate after damage [2]. Due to its high metabolic demand, the cochlea is particularly susceptible to oxidative stress induced by reactive oxygen species (ROS) [3]. ROS generation contributes to multiple pathways of apoptosis and necrotic cell death within auditory tissues and is the main cause of most types of SNHL [4]. The main structures damaged by ROS are the organs of Corti (OC), the stria vascularis, and spiral ganglia. The most important cells in the OC are hair cells, which are crucial for converting sound from mechanical motion signals to recognizable electrical signals in the brain. A large number of experiments focusing on oxidative stress have drawn attention to the protective function of antioxidant defense in SNHL [5]. However, there is still a lot of room for exploration in this area.

Thioredoxin-interacting protein (TXNIP) is a multifunctional protein, also known as thioredoxin binding protein-2 or vitamin D3 upregulated protein 1, which is a crucial negative modulator in the redox system, binds to thioredoxin (TRX) to inhibit the antioxidant activity of TRX, thereby causing cellular oxidative stress [6]. TXNIP is associated with oxidative stress and inflammation in many diseases, such as diabetes and its complications [7], neurodegenerative diseases [8], cancers [9], and cerebrovascular diseases [10]. However, TXNIP has rarely been associated with SNHL. Cisplatin-induced NOD-like receptor protein 3 (NLRP3) inflammasome activation-mediated pyroptosis has been reported to be alleviated by the downregulating of TXNIP in marginal cells, suggesting that TXNIP positively regulates NLRP3 inflammasome activation [11]. Nuclear factor-kappa B (NF- $\kappa$ B) is a pro-inflammatory transcription factor that can be used by TXNIP to promote inflammatory gene expression through chromatin modification and nuclear translocation of NF- $\kappa$ B [12]. In diabetic retinopathy, TXNIP activation leads to NF- $\kappa$ B activation, which in turn increases the production of inflammatory factors. Suppression of the TXNIP/NF- $\kappa$ B pathway inhibits inflammatory factors and restores tight connections between endothelial cells [13]. However, neither the TXNIP/NLRP3 nor the TXNIP/NF- $\kappa$ B pathway has been reported in SNHL.

Currently, there is no evidence suggesting that TXNIP is a therapeutic target for combating oxidative stress-induced damage in hair cells. In this study, we simulated oxidative stress damage in HEI-OC1 cells by treatment with H<sub>2</sub>O<sub>2</sub>. We used small interfering RNAs (siRNAs) to regulate the expression of TXNIP, and we assayed the expression of related molecules to explore the role and mechanism of TXNIP in hair cell degeneration under oxidative stress. Our findings may provide new insights into the molecular mechanisms and potential therapeutic strategies for SNHL.

## 2. Methods and materials

### 2.1. Cell culture and hydrogen peroxide treatment of HEI-OC1 cells

The inner ear cell line HEI-OC1 was purchased from the UCLA Technology Development Group (Los Angeles, CA, United States) and cultured in Dulbecco's modified Eagle's medium supplemented with 10 % fetal bovine serum (Gibco, United States) and 50  $\mu$ g/ml ampicillin (Sangon Biotech, Shanghai) at 33 °C in a humidified 5 % CO<sub>2</sub> atmosphere. Upon reaching 70–80 % confluence after 24 h of culture, H<sub>2</sub>O<sub>2</sub> was added to the culture medium to induce oxidative stress.

### 2.2. Cell vitality assay

Each well of a 96-well plate contained five cultured HEI-OC1 cell clones. Following cell attachment, the HEI-OC1 cells were subjected to several treatments. As directed by the manufacturer, cells were treated and then incubated for 2 h at 37 °C with the Cell Counting Kit 8 (CCK-8) reagent (MCE, HY-K0301, Shanghai, China). The absorbance was recorded at 450 nm by microplate reader (Bio-Rad). Values were standardized to 100 % of untreated blank control cells.

### 2.3. Western blot analysis

HEI-OC1 cell samples were lysed using RIPA lysis buffer (Epizyme, PC101, Shanghai, China), protease inhibitor (Epizyme, GRF101, Shanghai, China) and phosphatase inhibitor (Epizyme, GRF102, Shanghai, China) for 30 min at 4 °C to extract total protein. Each protein concentration was assayed using the BCA Protein Quantification Kit (Epizyme, ZJ102, Shanghai, China). Equal quantities of protein samples were separated by 10 % or 12.5 % sodium dodecyl sulfate-polyacrylamide gel electrophoresis (Epizyme, PG212 and PG213, Shanghai, China), then transferred onto nitrocellulose membranes (Pall, 66485, USA). The membranes were blocked for 1 h at room temperature with 1xTBST containing 5 % non-fat milk (Sangon Biotech, Shanghai), then incubated with primary antibody (TXNIP, Cell Signaling Technology Cat# 14715, RRID:AB\_2714178; NLRP3, ServiceBio Cat# GB114320, RRID:AB\_3073726; Caspase-1, Santa Cruz Biotechnology Cat# sc-56036, RRID:AB\_781816; NF- $\kappa$ B p65, Cell Signaling Technology Cat# 8242, RRID:AB\_10859369; Phospho-NF- $\kappa$ B p65, Cell Signaling Technology Cat# 3033, RRID:AB\_331284; GAPDH, Proteintech Cat# 60004-1-Ig, RRID:AB\_2107436; Beta Actin, Proteintech Cat# 66009-1-Ig, RRID:AB\_2687938) at 4 °C overnight. After washing three times with 1 × TBST buffer, the membranes were incubated with secondary antibodies (HRP Goat Anti-Rabbit IgG(H + L), ABclonal Cat# AS014, RRID:AB\_2769854; HRP Goat Anti-Mouse IgG(H + L), ABclonal Cat# AS003, RRID:AB\_2769851) for 2 h at room temperature. Finally, the membranes were developed using Omni-ECL™ Femto Light Chemiluminescence Kit (Epizyme, SQ201, Shanghai, China) and

photographed using the ChemiDocXRS imaging system (Bio-Rad, CA, USA). The images were analyzed using ImageJ software (Bethesda, USA).

#### 2.4. Immunofluorescence microscopy

HEI-OC1 cells were fixed in paraformaldehyde (4 %) for 20 min, then washed in PBS two times. After permeabilizing the cell specimens in 0.5 % Triton X-100 solution for 1 h, they were blocked with 10 % normal goat serum for 1 h at room temperature. The samples were first incubated with the primary anti-TXNIP antibody (ABclonal, A9342, China) for 12 h at 4 °C, washed three times with PBS, and then incubated with a fluorescent secondary antibody Goat Anti-Rabbit IgG H + L (Alexa Fluor 488), (Abcam, ab150077, China) for 1 h at 37 °C in the dark. Finally, the cells were incubated with DAPI in the dark and immediately imaged.

#### 2.5. siRNA transfection

HEI-OC1 cells were transfected with TXNIP-siRNAs (RiboBio, Guangzhou, China) using Lipofectamine™ 3000 (Invitrogen, L3000001, USA), in accordance with the manufacturer's instructions. The transfection control was HEI-OC1 cells transfected with siRNA-negative control (siRNA-NC). The control group consisted of untreated HEI-OC1 cells. The transfection process takes 24 h.

#### 2.6. ROS measurement

Confocal Petri dishes were inoculated with HEI-OC1 cells. Once the cells were attached to the dishes, they were cultured for 20 min in the dark in 10 μmol/L DCFH-DA (Beyotime, S0033S, China) to detect total ROS and 500 nmol/L Mito-SOX Red (Thermo Fisher, M36007, USA) to mitochondrial ROS. The cells were incubated with Hoechst reagent (Beyotime, C1028, China) for 10 min, and images were acquired using a fluorescence microscope and processed using ImageJ software.

#### 2.7. JC-1

Cells were cultured in six-well plates, and each well was treated differently. Appropriate amount of JC-1 (200 μM) (MCE, HY-K0601, Shanghai, China) was brought to room temperature, 10 μL of JC-1 (200 μM) was added to the medium of each well at a

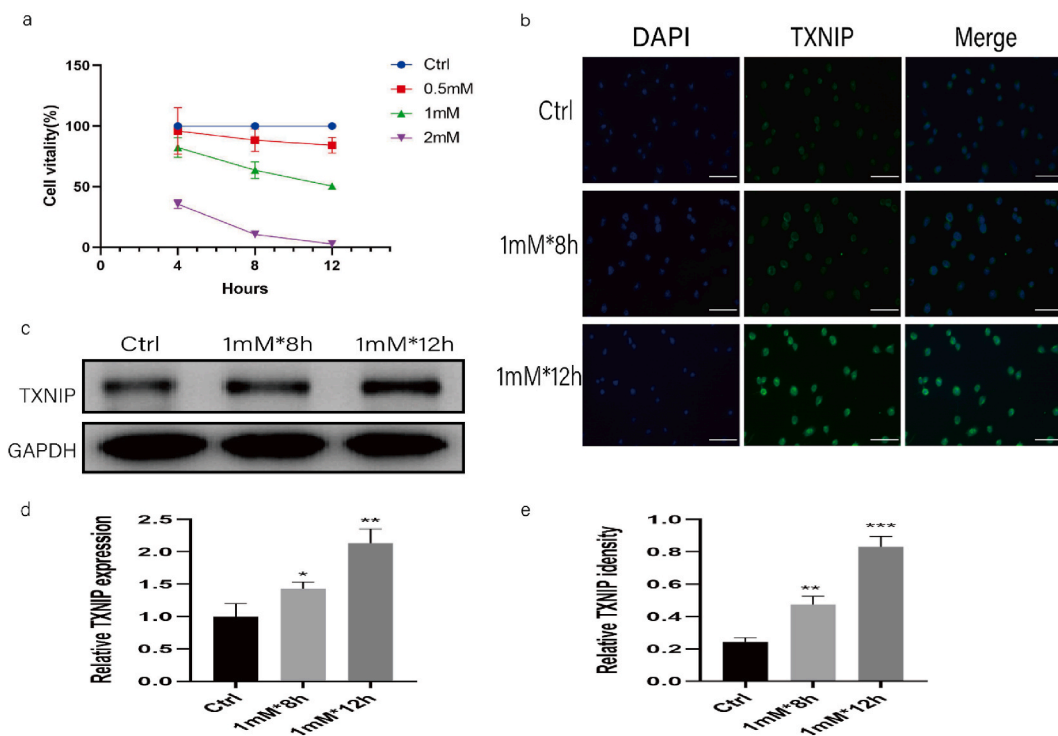


**Fig. 1.** Intracellular expression of TXNIP in HEI-OC1 at different times of 1 mM H<sub>2</sub>O<sub>2</sub> stimulation. (a) HEI-OC1 cell viability at 4, 8, and 12 h following stimulation with gradient concentrations of H<sub>2</sub>O<sub>2</sub> (0.5, 1, and 2 mM). (b) Immunofluorescence staining of TXNIP (green), and DAPI (blue) revealed the expression of TXNIP in HEI-OC1 cells at different stimulation times. (c) Western blotting showed the expression of TXNIP in different groups. Quantitative analysis of (d) Western blot and (e) immunofluorescence showed that 1 mM H<sub>2</sub>O<sub>2</sub> stimulation made a time-dependent increase in the intracellular content of TXNIP. \*p < 0.05, \*\*p < 0.01, \*\*\*p < 0.001 versus the control group. Scale bars = 50 μm.

final concentration of 2  $\mu$ M, and the cells were incubated at 37 °C in a cell culture incubator for 15–20 min. After incubation at 37 °C, the supernatant was aspirated, and the cells were washed with PBS (1  $\times$ ) for two times. Add 500  $\mu$ L of PBS (1  $\times$ ) and observe with a fluorescence microscope. The images were analyzed using ImageJ software (Bethesda, USA).

## 2.8. ELISA

Culture medium supernatants of six groups of cells with different treatments were collected, and IL-1 $\beta$  and IL-18 were detected in culture medium supernatants by ELISA kits according to the instructions (MULTI SCIENCES, EK201BHS/EK218-AW1, China). Dual-wavelength detection was performed using microplate reader (Bio-Rad) to determine the OD value at the 450 nm maximum absorption wavelength and the 630 nm reference wavelength. The calibrated OD value was the measured value at 450 nm minus the measured value at 630 nm.

## 2.9. Statistical analysis

The data are presented as mean and the standard deviation (SD), with each experiment repeated at least three times. Comparisons three or more groups were performed using one-way analysis of variance and Dunnett's multiple comparison test.  $P < 0.05$  indicates a statistically significant difference. SPSS software (version 22.0; IBM Corp, USA) was used for the statistical analysis and GraphPad Prism software (version 8.0.2, GraphPad Software Inc., USA) for constructing figure.

## 3. Results

### 3.1. Expression of TXNIP was upregulated in $H_2O_2$ -induced HEI-OC1 cells

We measured the vitality of HEI-OC1 cells after stimulation with different concentrations of  $H_2O_2$  at various times using CCK8 reagent (Fig. 1a), and we found that a concentration of 1 mM was appropriate; therefore, we used cells treated with 1 mM  $H_2O_2$  for 8 and 12 h. The expression of TXNIP was detected by immunofluorescence microscopy (Fig. 1b), and western blotting (Fig. 1c), showing a time-dependent increase compared to its expression in the untreated group ( $p < 0.05$ , Fig. 1d and e), suggesting that TXNIP is involved in oxidative stress in  $H_2O_2$ -induced HEI-OC1 cells.

### 3.2. TXNIP silencing ameliorated $H_2O_2$ -induced cell damage

To investigate whether silencing TXNIP could ameliorate cellular damage in an oxidative stress state, siRNA was used to knock-down TXNIP, as assessed by western blotting (Fig. 2a). CCK8 was used to assay cell viability (Fig. 2b). We observed a significant attenuation of the  $H_2O_2$ -induced decrease in cell viability after pretreatment of cells with siRNA-TXNIP ( $p < 0.01$ , Fig. 2b). TXNIP silencing ameliorated oxidative damage in HEI-OC1 hair cells.

### 3.3. Silencing TXNIP attenuated oxidative stress and mitochondrial dysfunction in $H_2O_2$ -induced HEI-OC1

TXNIP positively regulates ROS production. To investigate whether TXNIP silencing could reduce  $H_2O_2$ -induced total and mitochondrial ROS accumulation in HEI-OC1 cells, we used DCFH-DA to probe total ROS in the cells (Fig. 3a) and Mito-SOX to probe mitochondrial ROS (Fig. 3b). The phenomenon was that  $H_2O_2$  elevated the intracellular ROS ( $p < 0.001$ ) and mitochondrial ROS ( $p < 0.001$ ) levels, and silencing of TXNIP inhibited the increase of intracellular ROS ( $p < 0.001$ , Fig. 3c), which was also observed after incubation of the cells with Mito-SOX ( $p < 0.05$ , Fig. 3d). TXNIP silencing ameliorated cellular damage by attenuating oxidative stress

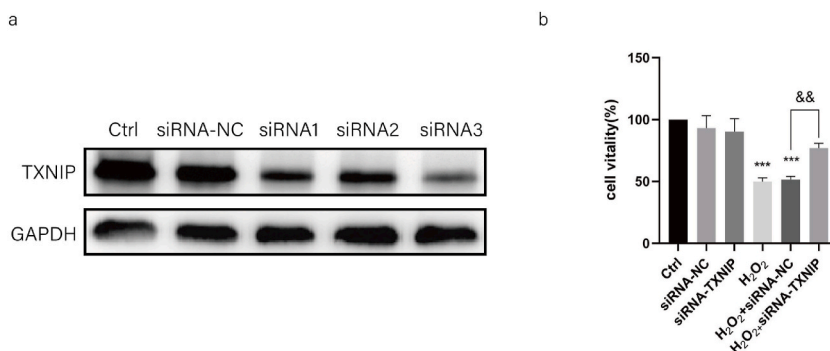
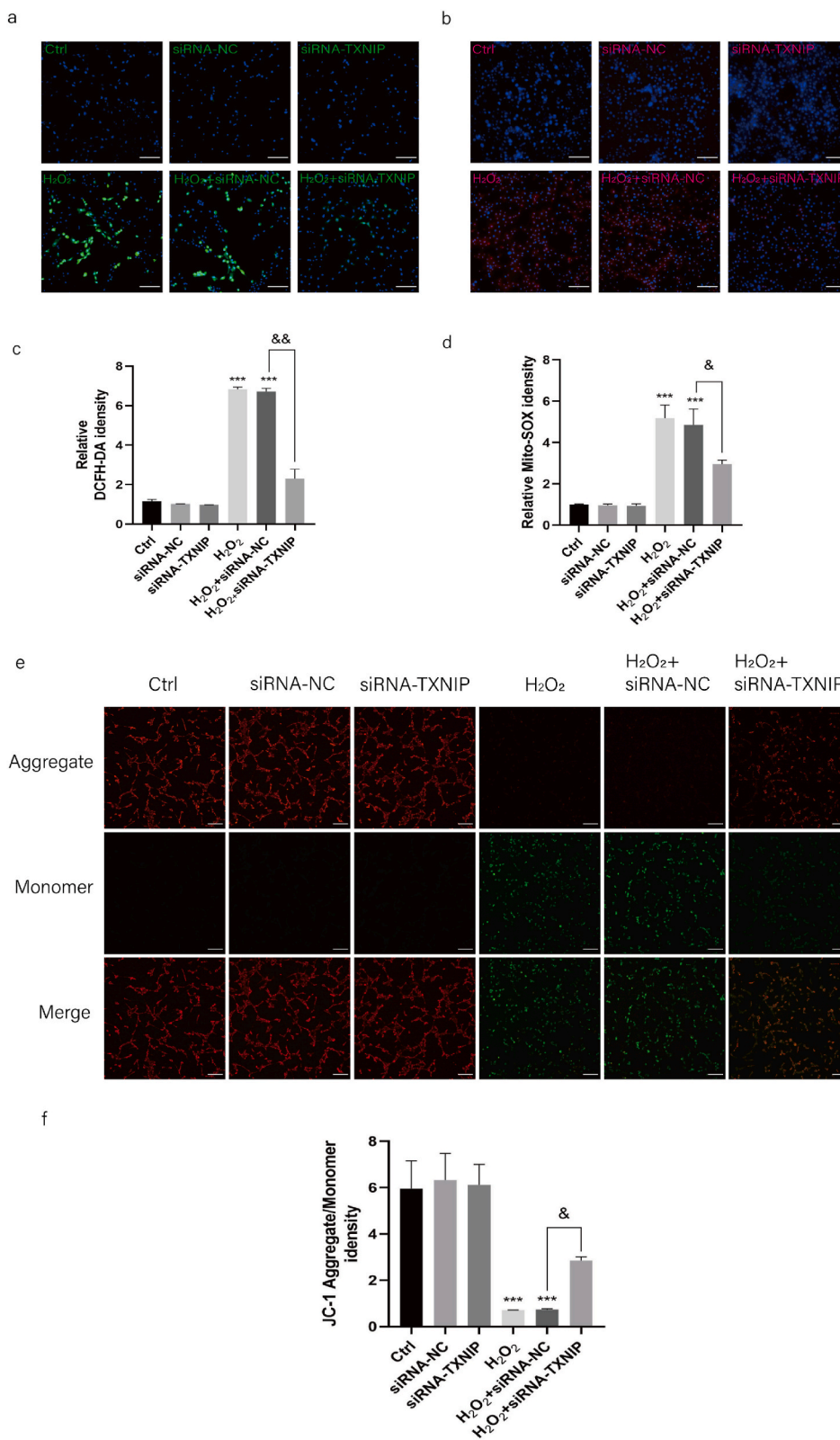


**Fig. 2.** Cell viability in different treatment groups. (a) Results of screening three potential siRNAs for knocking down TXNIP. (b) Effect of TXNIP knockdown on the vitality of HEI-OC1 cells treated with 1 mM  $H_2O_2$  for 12 h \*\*\* $p < 0.001$  versus the control group. &&  $p < 0.01$  versus the  $H_2O_2$ +siRNA-NC group.



(caption on next page)

**Fig. 3.** Effect of TXNIP knockdown on H<sub>2</sub>O<sub>2</sub>-induced ROS and MMP. (a) DCFH-DA-labelled total intracellular ROS of different groups (green). (b) Mito-SOX-labelled mitochondrial ROS of different groups (red). Quantitative analysis of (c) DCFH-DA and (d) Mito-SOX showing that TXNIP knockdown significantly reduced H<sub>2</sub>O<sub>2</sub>-stimulated intracellular and mitochondrial ROS accumulation. (e) JC-1 labelled MMP of different groups \*\*\*p < 0.001 versus the control group. & p < 0.05, && p < 0.01 versus the H<sub>2</sub>O<sub>2</sub>+siRNA-NC group. Scale bars = 200 μm.

and mitochondrial malfunction in HEI-OC1 cells.

To further illustrate the effect of silencing TXNIP on mitochondrial dysfunction, the JC-1 kit was used to assay mitochondrial membrane potential (MMP) (Fig. 3e). The MMP was significantly lower in the H<sub>2</sub>O<sub>2</sub> group compared with the ctrl group (p < 0.001), whereas the MMP was higher in the H<sub>2</sub>O<sub>2</sub>+siRNA-TXNIP group compared with the H<sub>2</sub>O<sub>2</sub>+siRNA-NC group (p < 0.05) (Fig. 3f). So silencing TXNIP ameliorated the H<sub>2</sub>O<sub>2</sub>-induced decrease in MMP.

### 3.4. Silencing TXNIP inhibited H<sub>2</sub>O<sub>2</sub>-induced NLRP3 inflammasome activation

TXNIP is involved in ROS-induced activation of NLRP3 inflammatory vesicles. To verify this, we examined NLRP3, pro-caspase-1, Cleaved-caspase-1 and pro-IL-18 levels by western blotting (Fig. 4a). NLRP3 (Fig. 4b) was significantly elevated in the H<sub>2</sub>O<sub>2</sub> (p < 0.01) and H<sub>2</sub>O<sub>2</sub> (siRNA-NC) groups (p < 0.01), and its levels in the H<sub>2</sub>O<sub>2</sub> (siRNA-NC) groups were higher than those in the H<sub>2</sub>O<sub>2</sub>-treated group with siRNA-TXNIP (p < 0.05). However, the opposite trend in pro-caspase-1 (p < 0.05, Fig. 4c) was related to the conversion of the precursor proteins into the activator form after stimulation. The trend of Cleaved-caspase-1 was similar to that of NLRP3 (p < 0.05 Fig. 4d) and the trend of pro-IL-18 (p < 0.05 Fig. 4e) was similar to that of pro-caspase-1. In addition, H<sub>2</sub>O<sub>2</sub> led to elevated IL-18 (p < 0.001) and IL-1β (p < 0.001), and silencing TXNIP inhibited this trend (p < 0.05) (Fig. 4f and g). Taken together, these results demonstrate that TXNIP silencing ameliorates oxidative damage in HEI-OC1 cells by inhibiting NLRP3 inflammatory vesicle activation.

### 3.5. Silencing TXNIP inhibited H<sub>2</sub>O<sub>2</sub>-induced NF-κB activation

To study the involvement of TXNIP in NF-κB activation, we measured the expression of the NF-κB's subunit p65 by western blotting (Fig. 5a). The results showed that the total p65 content remained unchanged (Fig. 5b), but phosphorylated p65 was significantly higher

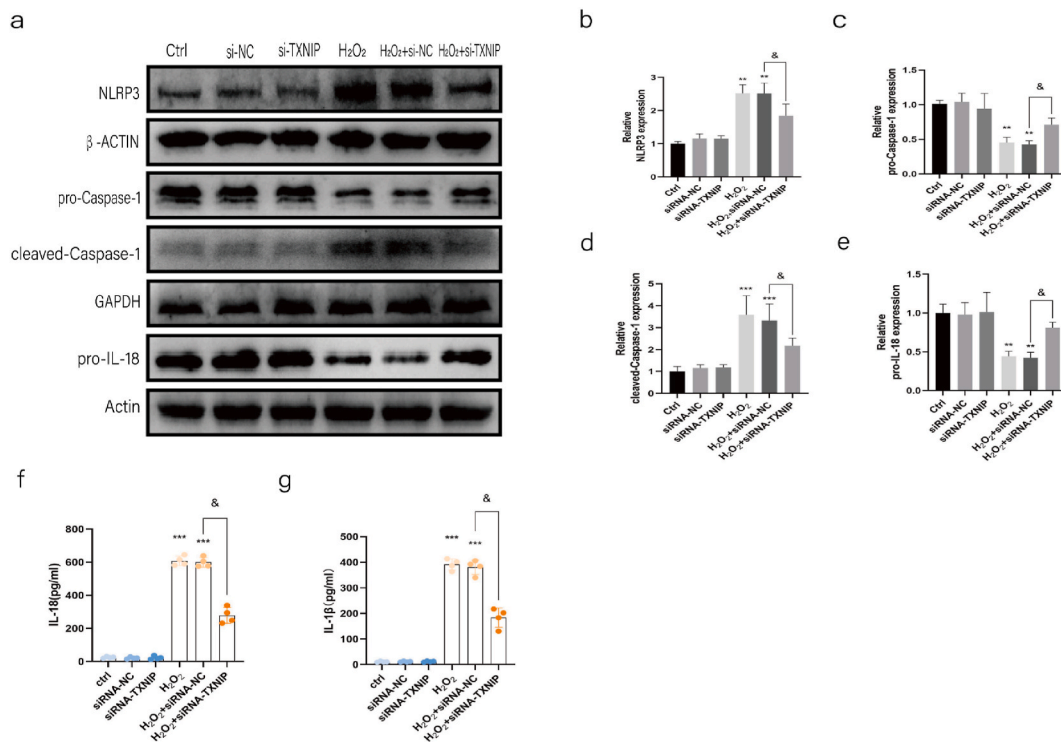


**Fig. 4.** Activation of NLRP3 inflammatory vesicles in different groups of HEI-OC1 cells. (a) Expression content of NLRP3, pro-caspase-1, Cleaved-caspase-1 and pro-IL-18 in different groups. Quantitative analysis of (b) NLRP3, (c) pro-caspase-1, (d) cleaved-caspase-1 and (e) pro-IL-18 showed that TXNIP knockdown inhibited H<sub>2</sub>O<sub>2</sub>-induced NLRP3 inflammatory vesicle activation. (f) The difference in the IL-18 concentrations in the supernatant of each group. (g) The difference in the IL-1β concentrations in the supernatant of each group. \*\*p < 0.01, \*\*\*p < 0.001 versus the control group. & p < 0.05 versus the H<sub>2</sub>O<sub>2</sub>+siRNA-NC group.

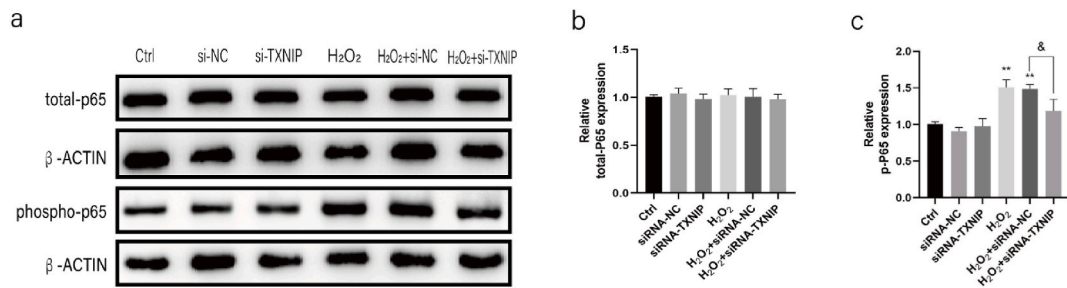


**Fig. 5.** NF- $\kappa$ B activation in different groups of HEI-OC1 cells. (a) Intracellular expression of total-p65 and phospho-p65 in different groups. Quantitative analysis of (b) total-p65 and (c) phospho-p65 showed that TXNIP knockdown inhibited H<sub>2</sub>O<sub>2</sub>-induced NF- $\kappa$ B activation. \*\* $p < 0.01$  versus the control group. &  $p < 0.05$  versus the H<sub>2</sub>O<sub>2</sub>+siRNA-NC group.

in the H<sub>2</sub>O<sub>2</sub>-treated group ( $p < 0.001$ ) and the H<sub>2</sub>O<sub>2</sub>-treated groups with negative control siRNA ( $p < 0.01$ ) than in the control group and was lower in the siRNA-TXNIP pretreated H<sub>2</sub>O<sub>2</sub> group than that in the siRNA-NC pretreated H<sub>2</sub>O<sub>2</sub> group ( $p < 0.05$ , Fig. 5c). We deduced that TXNIP silencing ameliorated oxidative damage caused by HEI-OC1 cells by inhibiting NF- $\kappa$ B activation.

#### 4. Discussion

In this study, we confirmed the role of TXNIP oxidative stress model in vitro. An imbalance between the generation of ROS and the capacity of the antioxidant defence system results in oxidative stress. In recent years, more and more studies on the regulation of TXNIP and ROS have been conducted. Multiple stimuli can induce intracellular ROS overproduction [14], including H<sub>2</sub>O<sub>2</sub>, and excessive ROS stimulate TXNIP to dissociate from TRX, causing elevation of TXNIP in the cell [15], TXNIP in turn positively regulates ROS [16]. In our study, accumulation of total and mitochondrial ROS in HEI-OC1 cells was observed after H<sub>2</sub>O<sub>2</sub> administration. It was also found that the increase in TXNIP content in HEI-OC1 cells treated with H<sub>2</sub>O<sub>2</sub> was time-dependent compared to the control group. After silencing TXNIP with siRNA targeting, ROS elevation and MMP decrease was inhibited and oxidative damage to hair cells was reduced. Our findings provide reliable preliminary research evidence for the scientific study that TXNIP may be a future target for the prevention and treatment of SNHL.

ROS-induced oxidative stress is a significant factor in multiple systemic and cochlear injuries. Previous research has shown that 40 min of low perfusion results in an average 10-fold increase in the concentration of hydroxyl radicals in the lymphatic vessels of the mouse cochlea, and that high levels of hydroxyl radicals can persist for 40–80 min after reperfusion [17]. The accumulation of superoxide and lipid peroxidation products can lead to apoptosis of cochlear cells, whereas vasoactive lipid peroxidation products can impair blood flow in the microcirculation, which further increases the production of ROS. This ultimately results in hair cell death via apoptosis and/or necrosis [18]. Mitochondria are the main sources of ROS, including superoxide anions, hydroxyl radicals, H<sub>2</sub>O<sub>2</sub> and singlet oxygen [19]. Excessive production of mitochondrial ROS in the cochlea can lead to oxidative degradation of major mitochondrial constituents, resulting in mitochondrial dysfunction and the inability of mitochondria to meet the high-energy needs of cochlear cells, leading to inadequate cellular bioenergy [20]. Inner and outer hair cells are the two most important sensory cells in the cochlea, and are important pathological targets in the occurrence of SNHL. Outer hair cells (OHCs) can endure prolonged high-energy requirements and mechanically induced stimuli, and they are inherently more susceptible to oxidative damage. The metabolic activity in the inner hair cells, stria vascularis, and spiral ganglion cells is also high, making them equally susceptible to mitochondrial dysfunction. Furthermore, dysfunctional mitochondria promote additional production of mitochondrial ROS through a positive feed-back pathway, eventually activating the cell apoptotic pathway and resulting in hearing loss [3].

TXNIP is involved in pro-inflammatory responses, such as activation of NLRP3 inflammasome and NF- $\kappa$ B. Under non-stress conditions, TXNIP binds to TRX, leading to the inactivation of NLRP3 inflammatory vesicles because of the absence of a mutual interaction between TXNIP and NLRP3. Nevertheless, during oxidative stress, ROS production induces TRX-TXNIP dissociation, which enhances NLRP3-TXNIP interaction [21]. The NLRP3 inflammasome is a crucial element of the human immune system, participates in multiple inflammatory pathways, mediating the activation of caspase-1 and the secretion of the pro-inflammatory cytokine IL-1 $\beta$ /IL-18 during microbial infections and in response to cellular damage [22]. Nevertheless, Abnormal activation of the NLRP3 inflammasome has been implicated in many inflammatory diseases [23].

Several studies on the inner ear have demonstrated the involvement of NLRP3 inflammatory vesicles in SNHL. Studies have found that NLRP3 expression is significantly higher in older mice than in younger mice [24], that noise exposure significantly up-regulates NLRP3 in the porcine cochlea [25], and that Pou4f3 knockout and exocytosis ameliorate cisplatin-induced ototoxicity in mice by reducing NLRP3 [26]. Similarly, in HEI-OC1, NLRP3 was found to be involved in cellular damage, in which BDE-47 impaired HEI-OC1 cellular activity by upregulating NLRP3 [27]. Although the important effects of NLRP3 in SNHL have been clarified, the studies on its upstream and downstream mechanisms are still few, and further refinement of the mechanism of NLRP3 occurrence in SNHL may help us to solve the disease. In our study, NLRP3, pro-caspase-1, Cleaved-caspase-1 and pro-IL-18 expression levels were evaluated in cells, IL-18, IL-1 $\beta$  in cells secretion, following various treatments. After H<sub>2</sub>O<sub>2</sub> treatment, the significant increase in NLRP3, Cleaved-caspase-1, IL-18 and IL-1 $\beta$  expression suggest the activation of NLRP3 inflammasomes in HEI-OC1 cochlear hair cells under oxidative stress, whereas the simultaneous decrease in pro-caspase-1 and pro-IL-18 was due to the conversion of precursor proteins

into active peptides under H<sub>2</sub>O<sub>2</sub> stimulation [28]. After TXNIP silencing, the expression of NLRP3, Cleaved-caspase-1, IL-18 and IL-1 $\beta$  decreased, whereas that of pro-caspase-1 and pro-IL-18 increased, indicating that the downregulation of TXNIP in HEI-OC1 cells inhibited the activation of NLRP3 inflammasomes induced by oxidative stress. Previous studies have found that knock down of TXNIP expression inhibits activation of the NLRP3 inflammasome in cochlear marginal cells treated with cisplatin, thereby alleviating oxidative stress damage to cochlear marginal cells [11]. Therefore, our results add data from a hair cell model on the targeting effects of TXNIP in cochlea. However, the direct binding of TXNIP to NLRP3 requires further investigation.

In the cochlea, ROS also interact with the NF- $\kappa$ B signalling pathway in a variety of ways, and the level of NF- $\kappa$ B activity is also affected by the level of ROS, which can produce pro-inflammatory mediators by activating the NF- $\kappa$ B signalling cascade [29]. Overexpression of NF- $\kappa$ B has been detected in in vivo models of noise-induced [30], and drug [31], and age-related hearing loss [32]. Previous studies have found that Asiaticoside ameliorates high glucose-induced oxidative stress damage in HEI-OC1 cells by inhibiting NF- $\kappa$ B [33]. The p65 subunit is an important component of NF- $\kappa$ B, and phosphorylation of p65 into the nucleus represents the activation of the NF- $\kappa$ B pathway. Total p65 levels are usually unchanged, whereas phosphorylated p65 levels increase upon NF- $\kappa$ B activation [34]. We examined the expression of total and phosphorylated p65 in each group of cells and found that the total p65 was essentially unchanged and phosphorylated p65 was significantly elevated after H<sub>2</sub>O<sub>2</sub> treatment. Simultaneous silencing of TXNIP prevents H<sub>2</sub>O<sub>2</sub>-stimulated p65 phosphorylation. This suggests that the NF- $\kappa$ B pathway is also activated after oxidative stress in HEI-OC1 cells, and that the inhibition of TXNIP overexpression prevents the activation of this pathway and exerts antioxidant and anti-inflammatory effects.

In conclusion, we addressed such ROS/NF- $\kappa$ B and ROS/NLRP3 pathway mechanisms in HEI-OC1 cells using TXNIP as an entry point, which may be a further refinement of the pathogenesis of SNHL. The results of the present study suggest that TXNIP is involved in oxidative damage in HEI-OC1 cochlear hair cells and that blocking TXNIP exerts anti-oxidative stress and anti-inflammatory effects by inhibiting both NLRP3 and NF- $\kappa$ B pathways. However, based on preliminary explorations with in vitro cell line models, further in vivo animal models are needed to validate whether targeted modulation of TXNIP is a possible new strategy in the field of antioxidant defence against SNHL.

#### Data availability statement

Data included in article/supp. material/referenced in article.

#### CRediT authorship contribution statement

**Ning Ma:** Writing – original draft, Methodology. **Liang Xia:** Formal analysis, Data curation. **Zhong Zheng:** Validation, Investigation. **Xiaoyan Chen:** Validation, Formal analysis. **Weiwei Xing:** Writing – review & editing, Project administration, Conceptualization. **Yanmei Feng:** Writing – review & editing, Project administration, Funding acquisition.

#### Declaration of competing interest

The authors declare the following financial interests/personal relationships which may be considered as potential competing interests: Yanmei Feng reports financial support was provided by National Natural Science Foundation of China. If there are other authors, they declare that they have no known competing financial interests or personal relationships that could have appeared to influence the work reported in this paper.

#### Acknowledgements

This research was funded by the National Natural Science Foundation of China (Nos. 8217040589 and 8237040716)

#### Appendix A. Supplementary data

Supplementary data to this article can be found online at <https://doi.org/10.1016/j.heliyon.2024.e37753>.

#### References

- [1] WHO, World report on hearing. <https://www.who.int/publications/i/item/9789240020481>, 2021. (Accessed 3 March 2021).
- [2] J.D.B. O'Sullivan, A. Bullen, Z.F. Mann, Mitochondrial form and function in hair cells, *Hear. Res.* 428 (2023) 108660. <http://10.1016/j.heares.2022.108660>.
- [3] W.J.T. Tan, L. Song, Role of mitochondrial dysfunction and oxidative stress in sensorineural hearing loss, *Hear. Res.* 434 (2023) 108783. <http://10.1016/j.heares.2023.108783>.
- [4] T. Kamogashira, C. Fujimoto, T. Yamasoba, Reactive oxygen species, apoptosis, and mitochondrial dysfunction in hearing loss, *BioMed Res. Int.* 2015 (2015) 617207. <http://10.1155/2015/617207>.
- [5] H. Ren, B. Hu, G. Jiang, Advancements in prevention and intervention of sensorineural hearing loss, *Ther Adv Chronic Dis* 13 (2022) 20406223221104987. <http://10.1177/20406223221104987>.
- [6] H.S. Park, J.W. Song, J.H. Park, et al., TXNIP/VDUP1 attenuates steatohepatitis via autophagy and fatty acid oxidation, *Autophagy* 17 (9) (2021) 2549–2564. <http://10.1080/15548627.2020.1834711>.



- [7] C.M. Osowski, T. Hara, B. O'Sullivan-Murphy, et al., Thioredoxin-interacting protein mediates ER stress-induced  $\beta$  cell death through initiation of the inflammasome, *Cell Metabol.* 16 (2) (2012) 265–273. <http://10.1016/j.cmet.2012.07.005>.
- [8] S. Ismael, Wajidunnisa, K. Sakata, M.P. McDonald, F.F. Liao, T. Ishrat, ER stress associated TXNIP-NLRP3 inflammasome activation in hippocampus of human Alzheimer's disease, *Neurochem. Int.* 148 (2021) 105104. <http://10.1016/j.neuint.2021.105104>.
- [9] J. Deng, T. Pan, Z. Liu, et al., The role of TXNIP in cancer: a fine balance between redox, metabolic, and immunological tumor control, *Br. J. Cancer* 129 (12) (2023) 1877–1892. <http://10.1038/s41416-023-02442-4>.
- [10] N. Li, H. Zhou, H. Wu, et al., STING-IRF3 contributes to lipopolysaccharide-induced cardiac dysfunction, inflammation, apoptosis and pyroptosis by activating NLRP3, *Redox Biol.* 24 (2019) 101215. <http://10.1016/j.redox.2019.101215>.
- [11] W. Yu, S. Zong, P. Zhou, et al., Cochlear marginal cell pyroptosis is induced by cisplatin via NLRP3 inflammasome activation, *Front. Immunol.* 13 (2022) 823439. <http://10.3389/fimmu.2022.823439>.
- [12] L. Perrone, T.S. Devi, K. Hosoya, T. Terasaki, L.P. Singh, Thioredoxin interacting protein (TXNIP) induces inflammation through chromatin modification in retinal capillary endothelial cells under diabetic conditions, *J. Cell. Physiol.* 221 (1) (2009) 262–272. <http://10.1002/jcp.21852>.
- [13] L. Tang, C. Zhang, Q. Yang, et al., Melatonin maintains inner blood-retinal barrier via inhibition of p38/TXNIP/NF- $\kappa$ B pathway in diabetic retinopathy, *J. Cell. Physiol.* 236 (8) (2021) 5848–5864. <http://10.1002/jcp.30269>.
- [14] A. Rimessi, M. Previati, F. Nigro, M.R. Wiecekowski, P. Pinton, Mitochondrial reactive oxygen species and inflammation: molecular mechanisms, diseases and promising therapies, *Int. J. Biochem. Cell Biol.* 81 (Pt B) (2016) 281–293. <http://10.1016/j.biocel.2016.06.015>.
- [15] G. Wu, S. Li, G. Qu, et al., Genistein alleviates H(2)O(2)-induced senescence of human umbilical vein endothelial cells via regulating the TXNIP/NLRP3 axis, *Pharm. Biol.* 59 (1) (2021) 1388–1401. <http://10.1080/13880209.2021.1979052>.
- [16] T. Bedarida, A. Domingues, S. Baron, et al., Reduced endothelial thioredoxin-interacting protein protects arteries from damage induced by metabolic stress in vivo, *Faseb. J.* 32 (6) (2018) 3108–3118. <http://10.1096/fj.201700856RRR>.
- [17] M.D. Seidman, W.S. Quirk, N.A. Shirwany, Mechanisms of alterations in the microcirculation of the cochlea, *Ann. N. Y. Acad. Sci.* 884 (1999) 226–232. <http://10.1111/j.1749-6632.1999.tb08644>.
- [18] T.M. Nicotera, B.H. Hu, D. Henderson, The caspase pathway in noise-induced apoptosis of the chinchilla cochlea, *J Assoc Res Otolaryngol* 4 (4) (2003) 466–477. <http://10.1007/s10162-002-3038-2>.
- [19] Y. Liu, M. Wei, X. Mao, T. Chen, P. Lin, W. Wang, Key signaling pathways regulate the development and survival of auditory hair cells, *Neural Plast.* 2021 (2021) 5522717. <http://10.1155/2021/5522717>.
- [20] E.C. Böttger, J. Schacht, The mitochondrion: a perpetrator of acquired hearing loss, *Hear. Res.* 303 (2013) 12–19. <http://10.1016/j.heares.2013.01.006>.
- [21] S.N. Harper, P.D. Leidig, F.M. Hughes Jr., H. Jin, J.T. Purves, Calcium pyrophosphate and monosodium urate activate the NLRP3 inflammasome within bladder urothelium via reactive oxygen species and TXNIP, *Res. Rep. Urol.* 11 (2019) 319–325. <http://10.2147/rru.S225767>.
- [22] T. Murakami, J. Ockinger, J. Yu, et al., Critical role for calcium mobilization in activation of the NLRP3 inflammasome, *Proc Natl Acad Sci U S A* 109 (28) (2012) 11282–11287. <http://10.1073/pnas.1117765109>.
- [23] G.E. Gregory, K.J. Munro, K.N. Couper, O.N. Pathmanaban, D. Brough, The NLRP3 inflammasome as a target for sensorineural hearing loss, *Clin Immunol* 249 (2023) 109287. <http://10.1016/j.clim.2023.109287>.
- [24] X. Shi, S. Qiu, W. Zhuang, et al., NLRP3-inflammasomes are triggered by age-related hearing loss in the inner ear of mice, *Am J Transl Res* 9 (12) (2017) 5611–5618.
- [25] N. Sai, Y.Y. Yang, L. Ma, et al., Involvement of NLRP3-inflammasome pathway in noise-induced hearing loss, *Neural Regen Res* 17 (12) (2022) 2750–2754. <http://10.4103/1673-5374.339499>.
- [26] R. Yu, K. Wang, W. Luo, H. Jiang, Knockdown and mutation of Pou4f3 gene mutation promotes pyroptosis of cochleae in cisplatin-induced deafness mice by NLRP3/caspase-3/GSDME pathway, *Toxicology* 482 (2022) 153368. <http://10.1016/j.tox.2022.153368>.
- [27] J. Tang, B. Hu, H. Zheng, et al., 2,2',4,4'-Tetrabromodiphenyl ether (BDE-47) activates Aryl hydrocarbon receptor (AhR) mediated ROS and NLRP3 inflammasome/p38 MAPK pathway inducing necrosis in cochlear hair cells, *Ecotoxicol. Environ. Saf.* 221 (2021) 112423. <http://10.1016/j.ecoenv.2021.112423>.
- [28] J. Lv, X. Shen, X. Shen, et al., NPLC0393 from *Gynostemma pentaphyllum* ameliorates Alzheimer's disease-like pathology in mice by targeting protein phosphatase magnesium-dependent 1A phosphatase, *Phytother Res.* 37 (10) (2023) 4771–4790. <http://10.1002/ptr.7945>.
- [29] A.R. Fetoni, F. Paciello, R. Rolesi, G. Paludetti, D. Troiani, Targeting dysregulation of redox homeostasis in noise-induced hearing loss: oxidative stress and ROS signaling, *Free Radic. Biol. Med.* 135 (2019) 46–59. <http://10.1016/j.freeradbiomed.2019.02.022>.
- [30] G. Zhang, H. Zheng, I. Pyykko, J. Zou, The TLR-4/NF- $\kappa$ B signaling pathway activation in cochlear inflammation of rats with noise-induced hearing loss, *Hear. Res.* 379 (2019) 59–68. <http://10.1016/j.heares.2019.04.012>.
- [31] C.H. Lee, K.W. Kim, S.M. Lee, S.Y. Kim, Dose-dependent effects of resveratrol on cisplatin-induced hearing loss, *Int. J. Mol. Sci.* 22 (1) (2020). <http://10.3390/ijms22010113>.
- [32] K. Uruguchi, Y. Maeda, J. Takahara, et al., Upregulation of a nuclear factor-kappa B-interacting immune gene network in mice cochleae with age-related hearing loss, *PLoS One* 16 (10) (2021) e0258977. <http://10.1371/journal.pone.0258977>.
- [33] Y. Xing, Q. Ji, X. Li, et al., Asiaticoside protects cochlear hair cells from high glucose-induced oxidative stress via suppressing AGEs/RAGE/NF- $\kappa$ B pathway, *Biomed. Pharmacother.* 86 (2017) 531–536. <http://10.1016/j.biopha.2016.12.025>.
- [34] A. He, J. Shao, Y. Zhang, H. Lu, Z. Wu, Y. Xu, CD200Fc reduces LPS-induced IL-1 $\beta$  activation in human cervical cancer cells by modulating TLR4-NF- $\kappa$ B and NLRP3 inflammasome pathway, *Oncotarget* 8 (20) (2017) 33214–33224. <http://10.18632/oncotarget.16596>.